Nuclear Instruments and Methods in Physics Research A 701 (2013) 235–242

Contents lists available at SciVerse ScienceDirect

Nuclear Instruments and Methods in Physics Research A

journal homepage: www.elsevier.com/locate/nima

Fast timing study of a $CeBr_3$ crystal: Time resolution below 120 ps at ^{60}Co energies

L.M. Fraile *, H. Mach [1], V. Vedia, B. Olaizola, V. Paziy, E. Picado, J.M. Udías

Grupo de Física Nuclear, Facultad de CC. Físicas, Universidad Complutense, CEI Moncloa, 28040 Madrid, Spain

ARTICLE INFO

Article history:
Received 25 May 2012
Received in revised form
18 October 2012
Accepted 2 November 2012
Available online 9 November 2012

Keywords:
Fast timing
$CeBr_3$
Inorganic scintillators
Time resolution
Fast photomultiplier tubes
Photonis XP20D0
Hamamatsu R9779

ABSTRACT

We report on the time response of a novel inorganic scintillator, $CeBr_3$. The measurements were performed using a cylindrical crystal of 1-in. in height and 1-in. in diameter at ^{22}Na and ^{60}Co photon energies. The time response was measured against a fast reference BaF_2 detector. Hamamatsu R9779 and Photonis XP20D0 fast photomultipliers (PMTs) were used. The PMT bias voltages and Constant Fraction Discriminator settings were optimized with respect to the timing resolution. The Full Width at Half Maximum (FWHM) time resolution for an individual $CeBr_3$ crystal coupled to Hamamatsu PMT is found here to be as low as 119 ps at ^{60}Co energies, which is comparable to the resolution of 107 ps reported for $LaBr_3(Ce)$. For 511 keV photons the measured FWHM time resolution for $CeBr_3$ coupled to the Hamamatsu PMT is 164 ps.

1. Introduction

The measurement of absolute nuclear transition probabilities is a very sensitive tool to study the structure of an atomic nucleus. Direct access to transition rates can be achieved via the lifetimes of nuclear levels de-populated in radioactive decay. The Advanced Time-Delayed (ATD) method, or Fast Timing [1,2], is a well-established technique to measure lifetimes ranging from 5 ps to 50 ns with count rates as low as 5 decays per second. The development of the technique was originally based on the use of Barium difluoride (BaF_2) inorganic crystals with excellent time response, on the introduction of photomultiplier anode timing, and on the combination of the fast BaF_2 scintillators with high-resolution HPGe detectors to provide a good energy selection [3].

Recently, a major breakthrough occurred with the introduction of the $LaBr_3(Ce)$ scintillator [4], which unites very good time response with energy resolution of the order of 3% at 662 keV, much superior to 9% for BaF_2 crystals. Better energy resolution provides an advantage in fast timing measurements where one has to disentangle complex decay schemes in which many transitions have similar, and thus overlapping energies. Furthermore, a better energy resolution gives a higher ratio between the full-energy peak and the Compton continuum underneath, and thus results in smaller time corrections due to Compton background under the full-energy peaks [3]. The time resolution of $LaBr_3(Ce)$ crystals is worse by about 10% to 15% than for BaF_2 crystals of the same size and shape. However, it has been reported that the time resolution of $LaBr_3(Ce)$ crystals depends on the amount of Ce doping [5] and improves with higher doping. Standard crystals commercially available at present have only 5% doping.

In the fast timing measurements performed over the last six years we have used three types of $LaBr_3(Ce)$ crystals: cylindrical in shape with the diameter and height of 1 in. × 1 in. and 1.5 in. × 1.5 in. and conical with the base diameter and height of 1.5 in. × 1.5 in., see for example [6]. Crystals were coupled to the Photonis fast-response 2-in. photomultiplier tubes XP20D0, which include a screening grid at the anode. These linear focused 8-stage XP20D0 PMT's [7] were operated at a high voltage value of only 900–980 V in order to avoid a strong deterioration of energy linearity. This is caused by the very high light yield of $LaBr_3(Ce)$ - crystals giving space charge effects in the photomultipliers.

The 8-stage Hamamatsu R9779 PMT is an alternative option for a 2-in. fast-response phototube. This unit includes an acceleration ring at the front-end and its timing properties have already been tested with plastic scintillators and small LSO crystals [8]. A comparison of selected timing properties of both

* Corresponding author. Tel.: +34 91 394 4784.
E-mail addresses: fraile@nuc2.fis.ucm.es, Luis.Fraile@cern.ch (L.M. Fraile).
URLS: http://nuclear.fis.ucm.es (L.M. Fraile), http://www.masticon.se (H. Mach).
[1] Permanent address: Medical and Scientific Time Imaging Consulting, MASTICON, Fruängsgatan 56 E, Nyköping 61130, Sweden.

0168-9002/$ - see front matter © 2012 Elsevier B.V. All rights reserved.
http://dx.doi.org/10.1016/j.nima.2012.11.009

phototubes coupled to $CeBr_3$ and $LaBr_3$(Ce) crystals was discussed in Ref. [9].

Our Fast Timing Array Collaboration plans to construct a large array of 50–60 fast timing detectors for the DESPEC experiments at the new FAIR facility [10]. The current plans call for the use of $LaBr_3$(Ce) detectors. Since $LaBr_3$(Ce) is an expensive crystal, there is a strong interest in cheaper alternatives. A viable alternative requires excellent time resolution and very good energy resolution matching $LaBr_3$(Ce) properties. The recently developed $CeBr_3$ scintillator is a very promising candidate due to its fast rise time of 0.7 ns, decay constant of 17 ns and high photon yield of about 68 000 photons/MeV [11–13]. Its peak emission wavelength is at 380 nm [14]. Importantly, at present this crystal is significantly less expensive. A good energy resolution, of the order of 4.3% at ^{137}Cs energy has been reported [15] for a 1-in. cylindrical $CeBr_3$ crystal but a poor time resolution of only 326 ps FWHM was measured for energies above 1050 keV. An important advantage of this crystal over BaF_2 or $LaBr_3$(Ce) is that it does not possess internal activity.

We report measurements of time response of a $CeBr_3$ crystal at the ^{22}Na and ^{60}Co photon energies. We also examine the energy resolution and linearity, which are relevant parameters for fast timing measurements.

2. Description of measurements

2.1. Experimental set-up for time-delayed measurements

The set-up for coincidence time-delayed measurements consisted of a reference detector with ultra-fast time response and the $CeBr_3$ detector under tests. The measurements of time resolution were performed with ^{60}Co and ^{22}Na γ-sources in a close geometry, with the detectors about 7 mm apart and the source positioned in-between them. Both detectors were coupled to standard NIM front-end electronics, as schematically depicted in Fig. 1. The anode signals from the PMT's were directly sent to ORTEC 935 Constant Fraction Discriminators, which were individually optimized for delay and walk (see Section 2.6). The output signals were taken to an ORTEC 567 TAC. The TAC amplitude signal, reflecting time difference between detector pulses, was sent to an ADC. The dynode outputs from both detectors provided the energy signals. Each signal was processed by an ORTEC 113 preamplifier and Tennelec TC247 spectroscopic amplifier before it was sent to an ADC. A logic signal generated for each valid TAC event was sent to the Gate and Delay Generator (GG) in order to provide gating signal to open the ADCs (see Fig. 1). List mode coincidence data from the three ADCs were stored on disk and analyzed off-line as described in Section 2.5.

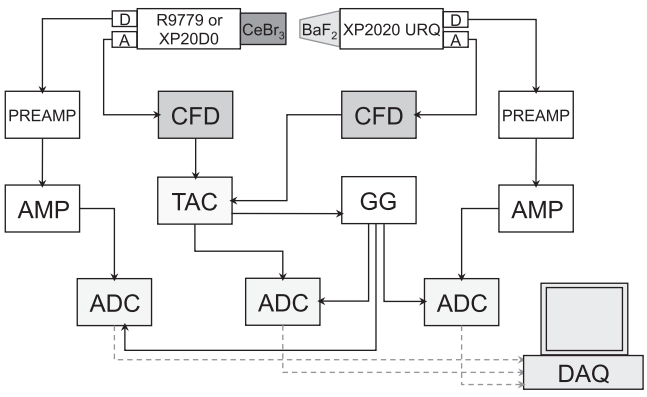

Fig. 1. Schematics of the time-delayed setup used to measure time response of the $CeBr_3$ crystal against the ultra-fast reference BaF_2 detector.

2.2. Reference BaF_2 detector

A small truncated cone BaF_2 crystal was used as a fast-response reference γ-detector. BaF_2 is still one of the fastest commercially produced inorganic crystal with the time resolution of the order 80 ps FWHM at ^{60}Co energies for small, about 1–2 cm^3, crystals, and up to 155 ps FWHM for large crystals of the Studsvik design [16]. The reference crystal was coupled to the Photonis XP2020-URQ PMT by means of Viscasil 60 000 cSt, a standard industrial silicon grease [17]. The photomultiplier was operated at 2300 V.

In order to determine the time response of the reference detector, a system of two identical BaF_2 crystals coupled to XP2020-URQ photomultipliers chosen with very similar parameters has been set up. The intrinsic resolution of the TAC and ADC electronics was measured to be of the order of 16 ps. The stability of the setup against short-term electronic drifts was monitored (see Section 2.5) and, if necessary, corrected for in the off-line analysis. All instability corrections were found to be below 2 ps.

Following the procedure for data analysis described in Section 2.6 the combined time resolution Full Width at Half Maximum (FWHM) at ^{60}Co energies for the set of two identical BaF_2 detectors was found to be 117 ± 2 ps, as shown in Fig. 2. After deconvolution, by assuming a Gaussian and identical time response for both detectors, the time resolution of an individual unit was 83 ± 2 ps. In the case of the 511-keV photons from a ^{22}Na source the deconvoluted response for each detector was 125 ± 2 ps. These values were used to deconvolute the unknown time resolution of $CeBr_3$ in our measurements. Note that the reference detector had a significantly smaller time resolution than our values reported for $CeBr_3$.

The performance and reproducibility of the time resolution of the reference BaF_2 detector was carefully monitored throughout the whole period of measurements which lasted a few months. Over this period a few timing checks were performed on the reference set of detectors. The monitoring measurements yielded time resolution for a single detector ranging from 81.5 ± 1.5 ps at the beginning of the measurements to 84.4 ± 1.5 ps for ^{60}Co at the end of them.

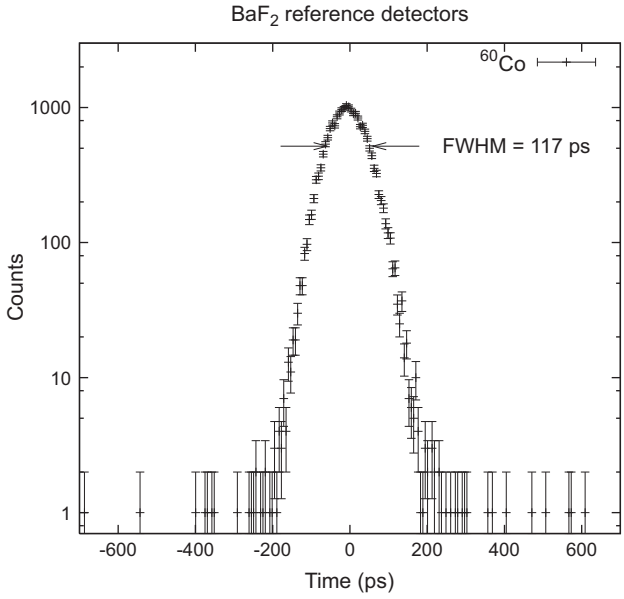

Fig. 2. Time spectrum for ^{60}Co generated by selecting full energy peak of γ rays detected in a pair of reference BaF_2 detectors. The time calibration is 6.0 ps per channel.

2.3. $CeBr_3$ crystal

The $CeBr_3$ crystal, with serial number SEW840, was produced by Scionix [18]. The cylindrical crystal of 1 in. in diameter and 1 in. in height was surrounded by reflector material and hermetically sealed at the factory with a quartz window in an aluminium case. The crystal was optically coupled by the use of a Viscasil silicon grease [17] to the Hamamatsu or Photonis photomultiplier tubes. A pre-delivery test at Scionix has shown the energy resolution of 4.2% at ^{137}Cs energy when coupled to Hamamatsu R6231 phototube operated at 880 V.

Upon delivery the front surface of the sealed crystal was smooth. However, a visual inspection after a few weeks of use has shown several spots, which looked like small bubbles formed between the crystal and the sealing optical glass. These spots covered about 5% of the crystal optical window after three weeks after delivery, but then increased to 7% over a few months period. If all the light reaching these spots were absorbed, then up to 7% of light collection from the crystal would be blocked.

2.4. Photomultipliers

XP20D0 is the fast-response 8-dynode phototube designed by Photonis to match the $LaBr_3$(Ce) crystals having a high yield of about 74 000 photons/MeV [5]. The front end does not follow the optimized design used in the XP2020-UR PMT, but instead used a simplified one. To improve the time resolution, these tubes are equipped with a double anode [7]. The XP20D0 has a typical rise time of 1.6 ns and a Transit Time Spread (TTS) of 520 ± 30 ps FWHM [7]. These are worse parameters than 1.4 ns and 350 ps, respectively, for the 12-stage XP2020-UR tubes. Two XP20D0/B tubes, with the serial numbers 2029 and 2156, were used in the tests. Their main properties are summarized in Table 1.

The Hamamatsu R9779 photomultiplier was incorporated into the assembly H10570 MOD with the serial number FA0472. This 52 mm 8-stage PMT was also designed for $LaBr_3$(Ce), and a typical anode pulse rise time of 1.8 ns and TTS of 250 ps FWHM were reported by the manufacturer [19]. The PMT properties are also summarized in Table 1.

Our standard procedure for setting a fast timing photomultiplier for nuclear structure experiments is to use the highest possible voltage limited by the energy non-linearity and the hardware constrains. In this study of the high photon-yield crystals, the high voltage on the photomultipliers was set to provide anode output signals of 1 V in amplitude for 1 MeV photons. Consequently the typical operation voltage was 1200 V for the XP20D0 and 1260 V for the R9779. The dependence of the FWHM time resolution and of other parameters on the high voltage applied to both types of phototubes was studied in this work and it is discussed further below.

Table 1
Summary of main properties of the photomultiplier tubes used in combination with the $CeBr_3$ crystal. Both XP20D0 and R9779 PMTs are 2-in. 8-stage linear focused photomultipliers with borosilicate glass window. The value for the R9779 PMT is given as blue sensitivity index for a Corning CS 5-58 blue filter [19].

PMT	s/n	τ_{rise} (ns)	FWHM TTS (ps)	Blue sensitivity (μA/lmF)	Dark current (nA)
XP20D0	2029	1.6	520 ± 30 [7]	12.0	2.3
XP20D0	2156	1.6	520 ± 30 [7]	11.6	1.13
R9779	FA0472	1.8	250 [19]	9.55*	1.40

2.5. Procedure of the data analysis; instability correction

The analysis of the list mode data was performed using the SORTM procedure described in Ref. [20]. Consequently, only a brief summary is given here. The data analyses for the sources of ^{60}Co and ^{22}Na are similar. In the case of ^{60}Co analysis, first broad energy windows are selected which include both the 1173- and 1332-keV peaks in the energy spectra on both detectors. Then a coincidence time spectrum is created for the selected energy events. Its FWHM and centroid position are determined for this total spectrum. Then the same selected data is sorted out again but this time it is subdivided into 6–10 consecutive data groups each giving at least 1000 events in its partial time spectrum. For each partial spectrum its FWHM and centroid are determined. The set of differences between the centroids of the partial spectra and the total spectrum reflects the pattern of instability shifts due to short-term drifts of electronics. These partial drifts were mostly below 1/2 of a channel, thus below 3 ps. In the next step the partial spectra were shifted (off-set shift) each by its position difference to the total spectrum and summed together.

For about 80% of the cases the instability correction was minor and the FWHM for the shifted summed spectrum was essentially the same as for the total uncorrected spectrum. In the remaining number of cases the correction produced small effects, below the sigma uncertainty of the measurement. Only in two cases when the corrections were significant, measurements were repeated.

The set of differences in the centroids of the partial spectra from the original total spectrum was preserved and applied again when the time resolution spectra ($CeBr_3$[1173]–BaF_2[1332]) and ($CeBr_3$[1332]–BaF_2[1173]) or ($CeBr_3$[511]–BaF_2[511]), discussed below, were sorted out. In these sortings the whole data set was subdivided into the same groups, partial time spectra were sorted out, evaluated, shifted by a discrete number of channels (if needed) and summed together.

2.6. Time resolution

The measurements of time resolution were performed with ^{60}Co and ^{22}Na γ-sources. In the case of ^{60}Co there are two full energy peaks at 1173 and 1332 keV recorded in each detector. Thus the time resolution represents an average value for two possible combinations of the peaks selected in the pair of detectors. In the first step, the full energy peak at 1332 keV was selected in one of the detectors (BaF_2) and the coincident 1173 keV peak was selected in the other one ($CeBr_3$). The energy gates were set roughly at the Full Width at Tenth Maximum (FWTM) of the energy peaks. Data corresponding to the selected energy events were sorted out and projected into a time spectrum (BaF_2[1332]–$CeBr_3$[1173]). The sorting included the instability corrections discussed above.

Next, the energy gates were reversed in the two detectors and a second time spectrum (BaF_2[1173]–$CeBr_3$[1332]) was created. Both time spectra have typically shown an approximately Gaussian symmetric shape, except when extreme parameters were set in the CFD, in which case the time spectra showed a small asymmetry on one side of the peak.

The centroid positions and FWHMs were determined for both time spectra. If their centroids differed significantly due to poor walk curve in the CFD, then one of them was shifted by a discrete number of channels in order to match the position of the other peak before these spectra were added together. This was done to remove the influence of the walk-curve on the reported time resolution of the detectors. In most cases reported here, only a marginal improvement (well below 2 ps) in the FWHM of the summed spectra was obtained by matching the positions of the

time spectra. The final time resolution FWHM was given for the summed spectrum.

In general the FWHM resolutions for the (1332–1173) and (1173–1332) time spectra are different, reflecting the fact that the time resolution for the $CeBr_3$ is significantly worse than for the reference crystals and that the time resolution depends on energy and deteriorates for lower energies.

In the case of ^{22}Na only one time spectrum, (BaF_2[511]–$CeBr_3$[511]), was sorted out by selecting the energy events on the peak at 511 keV. In this case the energy gates were set at the FWHM of the energy peaks.

2.7. Optimization of the time resolution

In order to find the optimum time resolution of $CeBr_3$ coupled to the fast-response PMTs we have measured the time resolution as a function of high voltage applied to the tube and two parameters of the CFD: the external delay and the walk adjustment (Z). The internal delay jumper on the ORTEC 935 CFD, W1, was removed throughout our measurements. According to the ORTEC user manual this setting corresponds to an internal delay of about -1 ns. The optimization process was iterative, by first finding a preliminary set of optimal parameters and then optimizing again using high precision measurements.

Throughout the measurements two fixed energy thresholds were simultaneously active on the $CeBr_3$ energy events. One was the lower energy discriminator on the ADC energy channel and the other was the CFD threshold. Since data were acquired in coincidence mode, which required a valid TAC signal to validate each event, the effect of thresholds was visible in the collected energy spectra. Only at the lowest value of high voltage applied to the PMT, the CFD threshold was higher than the ADC energy discriminator and then the low energy cutoff had the highest value of about 150 keV. For other high voltages the ADC energy discriminator determined the low energy cutoff. For example for the $CeBr_3$–Hamamatsu detector operated at HV=1330 V the low energy cutoff was about 50 keV.

2.8. Energy resolution

During the tests we have observed that a simple peak-sensing "MCA Box" multichannel analyzer by Leybold Didactic GmbH, controlled by a general purpose measurement program "CASSY", yields better energy resolution than the NIM modules described above, which were mainly designed for the HPGe detectors having signals with much longer decay times. Consequently, during the energy measurements and the determination of linearity, the dynode output of the $CeBr_3$ detector was directly send to the MCA Box. The use of preamplifiers did not provide any improvement.

We have examined the energy linearity as a function of the applied high voltage for the $CeBr_3$ crystal coupled to the Hamamatsu and the Photonis photomultipliers. The γ-ray energy range was from 122 to 1408 keV, while the high voltage range was from 1050 to 1400 V for the Hamamatsu PMT and from 850 to 1300 V for the Photonis tube.

2.9. Energy resolution and non-linearity

When the energy resolution is determined for crystals with high light output, like $LaBr_3$(Ce) or $CeBr_3$, care must be taken to account for the energy non-linearity caused by the space-charge effect in the photomultiplier tube and by the scintillator non-proportionality. For $CeBr_3$ the reported non-proportionality is 4% in the range from 122 to 1275 keV [11]. The procedure discussed below involves the determination of the functional relation between peak position (signal amplitude) and γ-ray energy.

The energy resolution, *ER*, is determined from the ratio of the FWHM of the full energy γ peak, here labelled ΔE, expressed in the units of energy, and the energy of the γ-ray peak, E_0

$$ER = \Delta E/E_0. \tag{1}$$

On the other hand, the parameters determined from the measured spectrum for the γ-ray of energy E_0 are the Δp (FWHM) and peak position, p_0, both expressed in ADC channels. An energy E_i is then given by a function $f(p)$ at the corresponding position p_i, $E_i = f(p_i)$. Assuming that to first order the transformation between energy and position is locally linear, the energy resolution can be derived from the relation

$$ER = \frac{\Delta p}{E_0} \times \left.\frac{df}{dp}\right|_{p=p_0}, \tag{2}$$

where the derivative is calculated at the point $p=p_0$. The function $f(p)$ describes the energy fit to a series positions of the of full energy peaks of known energies obtained by using a few different radioactive sources. For the energy determination we have used γ-sources of ^{137}Cs (662 keV), ^{60}Co (1173 and 1332 keV), ^{22}Na (511 keV), ^{152}Eu and ^{133}Ba where the γ-ray energies ranged from 122 to 1408 keV.

For a relatively small non-linearity, the energy relation $f(p)$ can be expressed by a second order polynomial, $f(p) = a+bp+cp^2$. By substituting this function into Eq. (2), *ER* can be expressed as

$$ER = \frac{b+2cp_0}{a+bp_0+cp_0^2}\Delta p. \tag{3}$$

A perfectly linear energy relation would have a zero offset and no quadratic term, thus $a=c=0$. Then the energy resolution becomes

$$ER = \Delta E/E_0 = \Delta p/p_0. \tag{4}$$

In reality the second equality in Eq. (4) is seldom true. For example, for the case of $CeBr_3$ with XP20D0 at 1000 V, taken from the measurements discussed further below, the coefficients for a quadratic fit are: $a=10.24$, $b=1.37$, and $c=0.00059$. Then the correct energy resolution at $E_0=662$ keV is $ER=5.0\%$, while the apparent energy resolution given by $\Delta p/p_0$ is 4.4%.

3. Results and discussion

3.1. Energy and linearity

An energy spectrum for the ^{137}Cs source obtained with the $CeBr_3$ crystal coupled to the XP20D0 photomultiplier operated at the voltage of 1200 V is plotted in Fig. 3. The FWHM value was corrected for non-linearity. The measured energy resolution at 662 keV is 5.0%. A similar value of 5.0% is obtained for the $CeBr_3$–Hamamatsu detector. These values are higher than 4.2% quoted by the manufacturer from the pre-delivery test at Scionix.

One should note that the fast-response phototubes have a special design, optimized for the time efficient collection of photoelectrons to arrive almost at the same time to the first dynode, in order to generate the output anode signals with the smallest TTS [21]. In particular, the XP20D0 PMT includes a screening grid at the anode [7] whereas the R9779 PMT has an acceleration ring at the front-end [19].

We have measured the energy linearity for the $CeBr_3$ crystal and the PMT combination as a function of high voltage applied to the photomultiplier. The results plotted in Fig. 4 show a very different behaviour for the tubes. The contribution from the non-proportionality in light yield of $CeBr_3$ is small. As stated above it

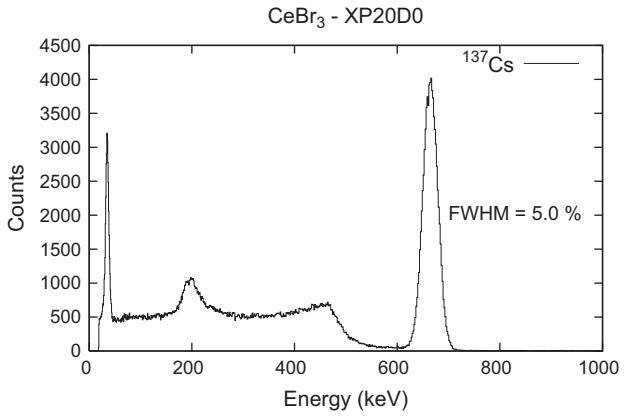

Fig. 3. Energy spectrum for $CeBr_3$ coupled to the Photonis XP20D0 PMT operated at HV=1200 V, for the ^{137}Cs source. The FWHM value was corrected for non-linearity.

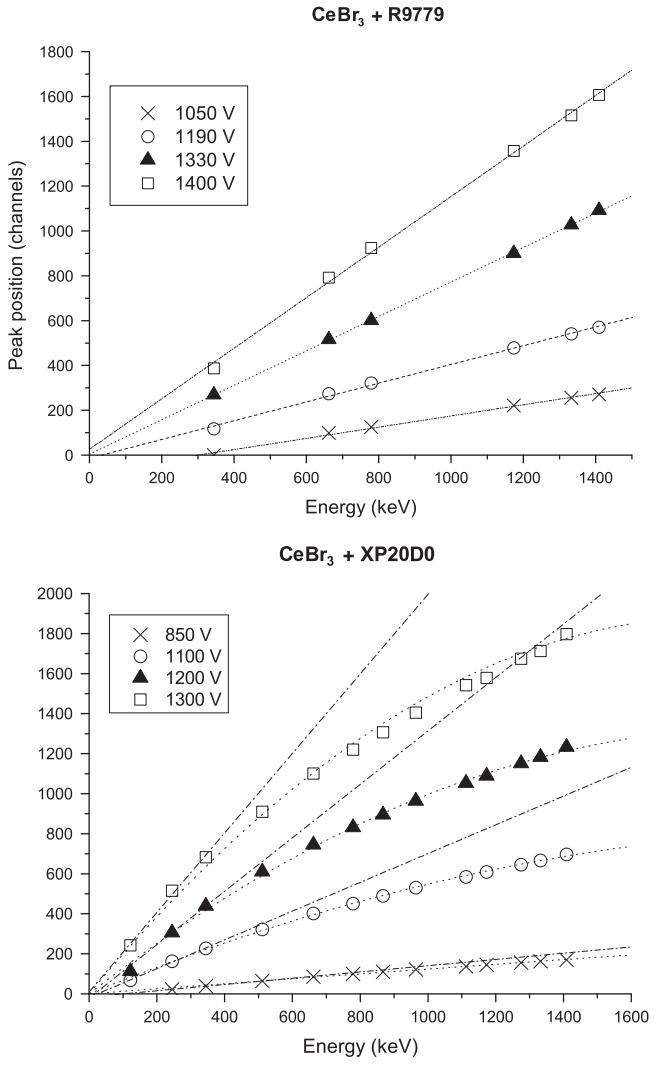

Fig. 4. Energy linearity plots for the $CeBr_3$ crystal coupled to the R9779 PMT (above) and XP20D0 PMT (below). The dynode signals are directly sent to an MCA without a preamplifier nor an amplifier. Signals for the lowest energies resulted in non-zero offset values. A linear fit is shown together with experimental points. Linear fits to the R9779 data are done over the full data range. For the XP20D0 the fits were performed for the points below 400 keV and then extrapolated to higher energies. The quadratic functions determined for the non-linearity correction are also plotted in this case.

has been measured [11] to be 4% in the range from 122 to 1275 keV and it is better than for other scintillators.

The R9779 PMT shows an almost linear energy relation over the whole energy range and for all high voltages applied in these tests. Particularly important is its good linearity at the voltage range about 1150–1350 V where the best time resolution is achieved (see Section 3.2).

There is a strong energy non-linearity observed for the $CeBr_3$ coupled to the XP20D0 PMT for the range of high voltages from 850 to 1400 V. The non-linearity is very strong at the operation voltage of 1200 V and increases with the applied voltage. This is shown in Fig. 4 by the departure from the linear fit, which was defined by the three lowest energies in the XP20D0 plot. Moreover, although the energy resolution at 662 keV is consistently 5.0% below 1200 V, it strongly deteriorates as the high voltage is further increased. In particular at 1800 V the pair of full energy peaks at 1173 and 1332 keV for ^{60}Co cannot be resolved anymore.

3.2. Time resolution

The time resolutions given here are for a single detector involving $CeBr_3$ and the Hamamatsu or Photonis phototubes, unless otherwise stated. As discussed in Section 2.7 there were two steps in the optimization process, which revealed strong differences in the responses of the two photomultipliers, namely the selection of an optimal external delay and measurements of the time response as a function of applied high voltage.

In the first step, we have examined the shapes of the fast negative anode pulses on a 4 GSa/s oscilloscope and determined the time it takes from 20% of the pulse to the maximum, which is suggested in the ORTEC CFD user manual to use as the initial time delay for the CFD. For $CeBr_3$ coupled to the Photonis XP20D0 tube this time was about 8 ns, while for the crystal coupled to the Hamamatsu tube the pulse was much faster with the time difference of only 5 ns. Sample traces from the oscilloscope are plotted in Fig. 5.

We have then measured the time resolution as a function of the external delay applied to the $CeBr_3$ CFD. Fig. 6 shows the results for both phototubes. In the case of the Hamamatsu tube the minimum time resolution was found at only 1.5 ns. A sharp minimum is clearly seen at the ^{60}Co energies as well as at the energy of 511 keV for the ^{22}Na source. The dependence for the Photonis tube is much weaker and the minimum is almost flat at about 5.5–6.0 ns.

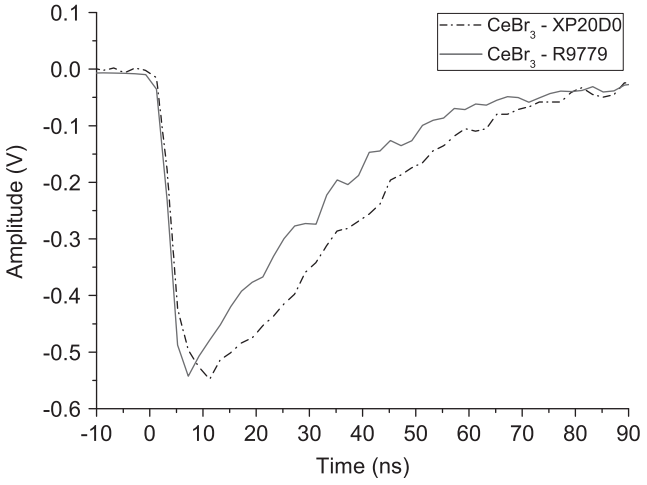

Fig. 5. Example of fast negative anode pulse for $CeBr_3$ coupled to Hamamatsu R9779 PMT and Photonis XP20D0.

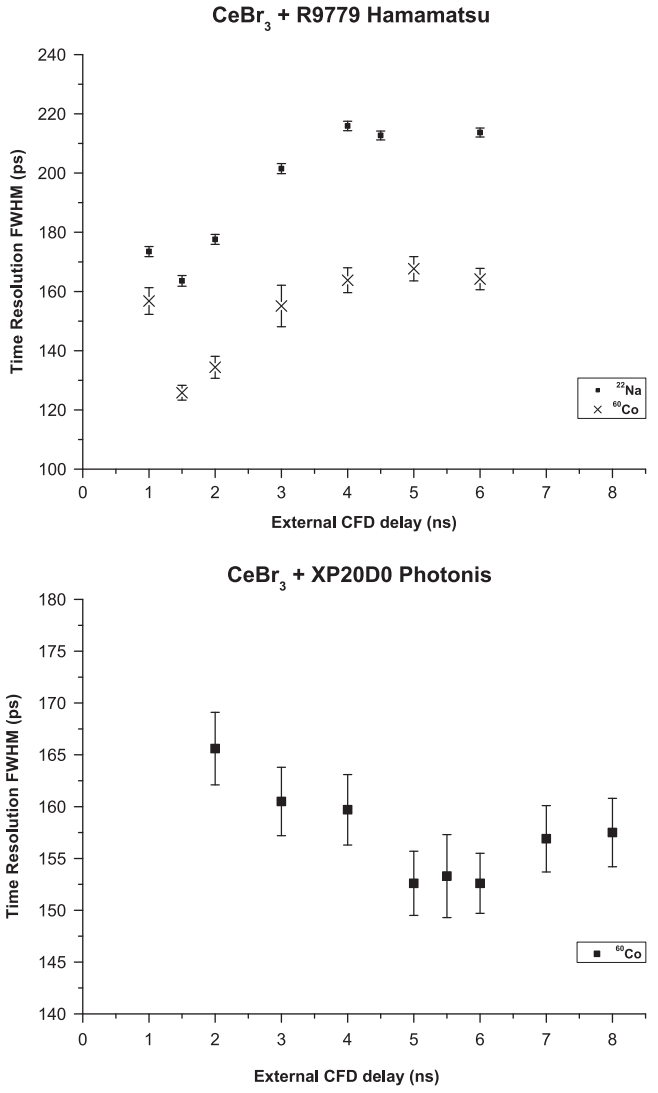

Fig. 6. Dependence of time resolution FWHM in ps as a function of the external delay in ns for an individual detector: $CeBr_3$ coupled to Hamamatsu R9779 PMT (top panel) and to Photonis XP20D0 (bottom panel). The internal delay jumper on the ORTEC 935 CFD, was removed, which corresponds to an internal delay of about −1 ns. The results were obtained using the sources of ^{60}Co (γ-ray energies of 1173 and 1332 keV) and ^{22}Na (at 511 keV).

Based on these results we have selected the external CFD delays of 1.5 ns and 6.0 ns for further test with the Hamamatsu and Photonis tubes, respectively. After optimizing the walk, which made only a small improvement of the order of 2 ps, we have examined the influence of applied high voltage on the time resolution. Our expectation was that with the increased high voltage the time resolution will first improve and then, when the gain will increase too much, space-charge effects will degrade the shape of the pulses. For a photomultiplier best suited for the application of $CeBr_3$ crystal to the timing γ spectroscopy, the minimum time resolution should occur at the same high voltage range where the energy resolution and linearity are at least acceptable.

The results are plotted in Fig. 7. For the Hamamatsu tube the time resolution steadily improves up to the voltage of 1300 V and then it remains rather steady with the minimum value of 119 ps at 1330 V. Operating the tube at higher voltages does not improve the performance for $CeBr_3$.

In contrast, the time resolution for the Photonis tube steadily improves with an increased high voltage until it saturates at very

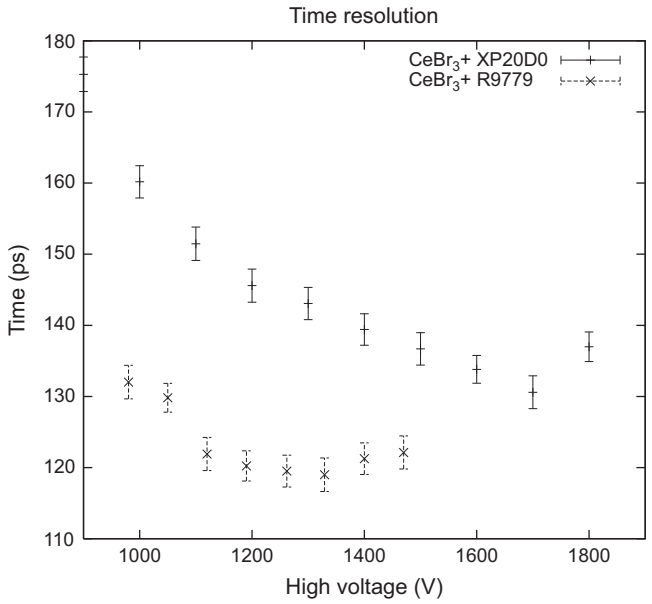

Fig. 7. Dependence of the FWHM time resolution in ps obtained for the $CeBr_3$ crystal coupled to the Hamamatsu R9779 and Photonis XP20D0 PMTs as a function of the applied high voltage. Results are given for an individual detector.

Table 2
Summary of FWHM time resolutions for the $CeBr_3$–Hamamatsu detector at HV = 1330 V and $CeBr_3$–Photonis detector at HV = 1200 V using sources of ^{60}Co (at 1173/1332 keV) and ^{22}Na (at 511 keV); see text for details.

Detector	^{60}Co (ps)	^{22}Na (ps)
$CeBr_3$–XP20D0	146 ± 2	210 ± 2
$CeBr_3$–R9779	119 ± 2	164 ± 2

high voltages, of the order of 1700 V, in a regime where the photomultiplier is no longer usable due to its extremely bad energy resolution and drastic non-linearity. In any case, the Photonis tube does not reach the excellent time resolution provided by the Hamamatsu tube. In the operational region for the Photonis tube, from 850 to 1200 V, even with strong non-linearity, its best time resolution is only 146–160 ps, thus well above the best value for Hamamatsu of 119 ps.

The FWHM time resolutions measured for the $CeBr_3$ crystal with both photomultipliers are summarized in Table 2. For the full energy peaks at ^{60}Co the resolution is 119 ± 2 ps for the $CeBr_3$ and R9779 combination at HV = 1330 V, whereas it is only 146 ± 2 ps for the crystal coupled to the XP20D0 at HV = 1200 V (at the highest bias voltage for which the energy non-linearity can be still acceptable in some applications). Although a better time resolution of 131 ± 2 ps is obtained for the latter detector at 1700 V, at that energy it does not provide any useful energy resolution nor linearity. For 511-keV photons from the ^{22}Na source the time resolution is 164 ± 2 ps for the $CeBr_3$ and Hamamatsu tube at 1330 V, and 210 ± 2 ps for the $CeBr_3$ and XP20D0 at HV = 1200 V. Time spectra for the $CeBr_3$ and R9779 combination are shown in Fig. 8.

Using a similar 1-in. $CeBr_3$ crystal coupled to a 10-stage Photonis XP6242B01 photomultiplier, an intrinsic FWHM time resolution of 326 ± 7 ps at ^{60}Co was reported in Ref. [15]. It is not clear to us why the former time resolution is almost three times worse than our result. On the other hand, an excellent FWHM time resolution of only 59 ps using the ^{22}Na source was reported [22] for a tiny $4 \times 4 \times 5$ mm^3 $CeBr_3$ crystal coupled to a Hamamatsu R4998 PMT, which is consistent with our data, since

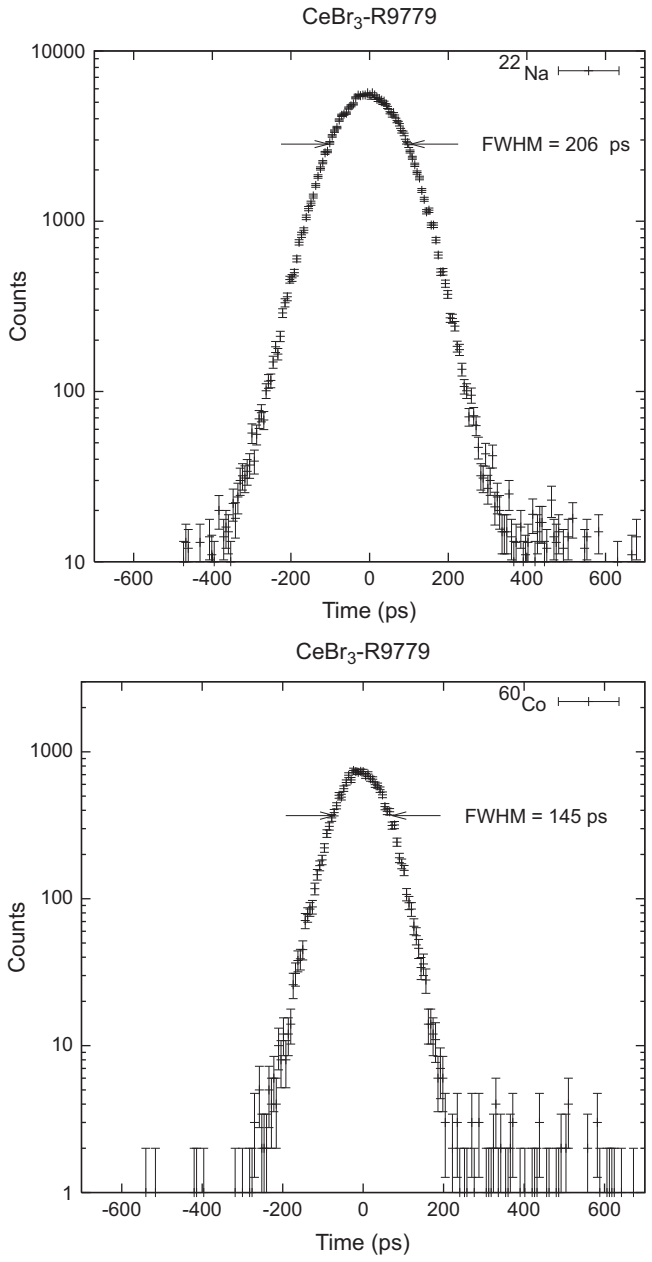

Fig. 8. Time spectrum for $CeBr_3$–Hamamatsu detector against the reference detector measured with a ^{22}Na source (top panel). The FWHM resolution of 206 ps includes individual contributions from the reference detector of 125 ± 2 ps and the $CeBr_3$ unit of 164 ± 2 ps. The bottom panel shows the time spectrum measured for the same detectors using a ^{60}Co source. Here the time resolution of 145 ps includes individual contributions from the reference detector of 83 ± 2 ps and the $CeBr_3$ unit of 119 ± 2 ps.

much improved time resolution is generally observed for smaller-size crystals. The crystal used in Ref. [22] has about 160 times smaller volume than the one used in our work. In the same work FWHM time resolutions at 511 keV of 173 ps and 210 ps were measured for a small $4 \times 4 \times 30\ mm^3$ $CeBr_3$ crystal coupled to a Hamamatsu R4998 PMT, and a Photonis XP20D0, respectively.

4. Summary and conclusions

We have studied the time response of a $CeBr_3$ crystal of 1 in. in diameter and 1 in. in height, commercially available from Scionix, with two 2-in. fast-response photomultipliers. The best results were obtained with the R9779 Hamamatsu phototube. Very good time resolutions of 119 ± 2 ps and 164 ± 2 ps were obtained at ^{60}Co energies and for 511 keV photons from a ^{22}Na source, respectively, for the $CeBr_3$–Hamamatsu detector operated at HV = 1330 V. The time resolution stays constant over the high voltage range from 1100 to 1450 V. At the operational voltage the response of the $CeBr_3$–Hamamatsu detector was very linear in energy, and good energy resolution was preserved. Based on our measurements it can be concluded that the Hamamatsu R9779 PMT is very well suited for this novel scintillator.

Measurements of the $CeBr_3$ crystal coupled to the Photonis XP20D0 photomultiplier have revealed a strong energy non-linearity and much worse time resolution. In the tests we have used two Photonis XP20D0 tubes, which have shown a similar behaviour. The XP20D0 phototubes have been shown to work very well with $LaBr_3$(Ce) crystals. In particular, an excellent time resolution of 107 ± 4 ps was reported [7] for a $LaBr_3$(Ce) cylindrical crystal of identical dimensions to the $CeBr_3$ studied here, and coupled to the XP20D0 photomultiplier.

In the present tests the XP20D0 and R9779 tubes have shown different time characteristics when coupled to the $CeBr_3$ crystal. This demonstrates how important it is to match individually the type of a photomultiplier to a specific class of fast high-yield crystals. The present results also prove that the novel $CeBr_3$ crystal is a strong competitor to $LaBr_3$(Ce) in fast timing applications. With similar energy and time resolution to $LaBr_3$(Ce), the $CeBr_3$ - crystal, having no internal activity, is more suitable than $LaBr_3$ (Ce) in applications where very low background activity is required, as for example in the fast timing nuclear spectroscopic studies of very exotic decays.

Acknowledgements

We kindly acknowledge support from Comunidad de Madrid (ARTEMIS S2009/DPI-1802), Complutense University (Grupos UCM, 910059), by CDTI under the CENIT Programme (AMIT Project), and from the Spanish Ministry of Science and Innovation (FPA2010-17142 and CPAN, Centro de Física de Partículas, Astropartículas y Nuclear, CSD-2007-00042, Ingenio2010). One of us (HM) would like to acknowledge the hospitality and support from the Grupo de Física Nuclear during his stay as CPAN Senior Expert at the University Complutense. The electronics for the testing bench and the reference detectors were provided by the Fast Timing Pool of Electronics and MASTICON.

References

[1] H. Mach, R.L. Gill, M. Moszyński, Nuclear Instruments and Methods in Physics Research A 280 (1989) 49.
[2] M. Moszyński, H. Mach, Nuclear Instruments and Methods in Physics Research A 277 (1989) 407.
[3] H. Mach, F. Wohn, G. Molnár, K. Sistemich, J.C. Hill, M. Moszyński, R. Gill, W. Krips, D. Brenner, Nuclear Physics A 523 (1991) 197.
[4] E.V. van Loef, P. Dorenbos, C.W.E. van Ejik, K. Krämer, H.U. Güdel, Nuclear Instruments and Methods in Physics Research A 486 (2002) 254.
[5] J. Glodo, W.W. Moses, W.M. Higgins, E.V. van Loef, P. Wong, S.E. Derenzo, M.J. Weber, K.S. Shah, IEEE Transactions on Nuclear Science NS-52 (5) (2005) 1805.
[6] E.R. White, H. Mach, L.M. Fraile, U. Köster, O. Arndt, A. Blazhev, N. Boelaert, M.J.G. Borge, R. Boutami, H. Bradley, N. Braun, Z. Dlouhy, C. Fransen, H.O.U. Fynbo, C. Hinke, P. Hoff, A. Joinet, A. Jokinen, Physical Review C 057303 (2007) 7.
[7] M. Moszyński, M. Gierlik, M. Kapusta, A. Nassalki, T. Szczesniak, M. Fonatine, P. Lavoute, Nuclear Instruments and Methods in Physics Research A 567 (2006) 31.
[8] F. Bauer, M. Aykac, M. Loope, C.W. Williams, L. Eriksson, M. Schmand, IEEE Transactions on Nuclear Science NS-54 (3) (2007) 422.
[9] L.M. Fraile, H. Mach, B. Olaizola, V. Paziy, E. Picado, J.J. Sanchez, J.M. Udias, J.J. Vaquero, V. Vedia, in: Nuclear Science Symposium Conference Record, 2011. NSS '11. IEEE, 2011, pp. 72–74.

[10] HIgh-Resolution In-flight SPECtroscopy/DEcay SPECtroscopy, FAIR, Facility for Antiproton and Ion Research. URL 〈http://www.fair-center.eu/public/experiment-program/nustar-physics/despechispec.html〉.
[11] K.S. Shah, J. Glodo, W. Higgins, E.V. van Loef, W.W. Moses, S.E. Derenzo, M.J. Weber, IEEE Transactions on Nuclear Science NS-52 (6) (2005) 3157.
[12] W. Drozdowski, P. Dorenbos, A. Bos, G. Bizarri, A. Owens, F. Quarati, IEEE Transactions on Nuclear Science NS-55 (3) (2008) 1391.
[13] P. Guss, M. Reed, D. Yuan, A. Reed, S. Mukhopadhyay, Nuclear Instruments and Methods in Physics Research, A 608 (2) (2009) 297.
[14] W. Higgins, A. Churilov, E. van Loef, J. Glodo, M. Squillante, K. Shah, Journal of Crystal Growth 310 (2008) 2085.
[15] R. Billnert, S. Oberstedt, E. Andreotti, M. Hult, G. Marissens, A. Oberstedt, Nuclear Instruments and Methods in Physics Research A 647 (2011) 94.
[16] H. Mach, L.M. Fraile, Hyperfine Interactions, in press. http://dx.doi.org/10.1007/s10751-012-0613-8.
[17] W. Klamra, T. Lindblad, M. Moszyński, L. Norlin, Nuclear Instruments and Methods in Physics Research A 254 (1) (1987) 85.
[18] SCIONIX Holland BV. URL 〈www.scionix.nl〉.
[19] Hamamatsu Photonics, Photomultiplier Tube R9779 Specifications, 2009.
[20] H. Mach, Instructions for the program SORTM. (Internal Report. Universidad Complutense, 2012).
[21] T. Szczesniak, M. Moszyński, L. Swiderski, A. Nassalski, P. Lavoute, M. Kapusta, IEEE Transactions on Nuclear Science NS-56 (1) (2009) 173.
[22] R.I. Wiener, M. Kaul, S. Surti, J.S. Karp, in: Nuclear Science Symposium Conference Record, 2010. NSS '10. IEEE, 2010, pp. 1991–1995.